Practical Considerations for GRAPPA-accelerated Readout-Segmented EPI in Diffusion-Weighted Imaging

S. J. Holdsworth[1], S. Skare[1], R. D. Newbould[1], A. Nordell[2], and R. Bammer[1]

[1]Department of Radiology, Stanford University, Palo Alto, CA, United States, [2]Hospital Physics, Karolinska University Hospital, Stockholm, Sweden

Introduction: Readout mosaic segmentation (RS-EPI) has been suggested as an alternative approach to EPI for high resolution diffusion-weighted imaging (DWI) with minimal geometric distortions (1). The RS-EPI trajectory must be coupled with the use of a second navigator echo to correct for shifts in *k*-space that occur during the application of the diffusion-encoding gradients. Larger shifts which displace the signal outside the *k*-space sampling range can cause dramatic signal loss. This effect can be minimized with the use of overlapping blinds, however this comes at the expense of scan time. In this abstract, peripherally cardiac gated and non-gated RS-EPI-DW images are acquired with the use of parallel imaging. To achieve a smaller effective TE, the blinds are acquired with Partial Fourier imaging. The methods used to phase correct and reconstruct the resulting data are described. The datasets are reconstructed with various overlapping factors to assess whether physiological motion significantly degrades the image quality. It is assessed whether the RS-EPI scan time can be reduced through the use of non-gated acquisitions with minimally overlapping blinds using a typical set of scan parameters we are using for high resolution DW acquisitions.

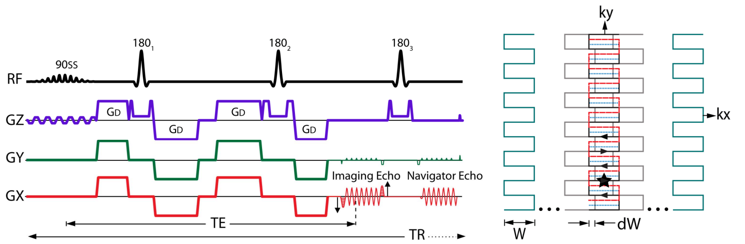

Figure 1: (left) Pulse sequence timing diagram for the RS-EPI, twice-refocused spin echo-based diffusion sequence. The RF pulses (spectral-spatial 90º and refocusing 180º); the diffusion gradients G_D; and the imaging and navigator echo are shown. (right) Resulting *k*-space, filled with an odd number of separate blinds, *B*, (indicated by green, grey, and black) of a given blind width, *W*, and overlapping factor, *OF* = *dW/W*. A fully sampled central blind (interleaved black, red, and blue trajectories) is used to get the ghost calibration parameters and GRAPPA weights, which are applied to all other blinds.

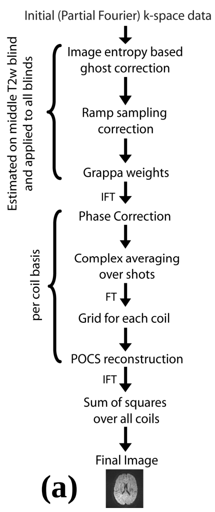

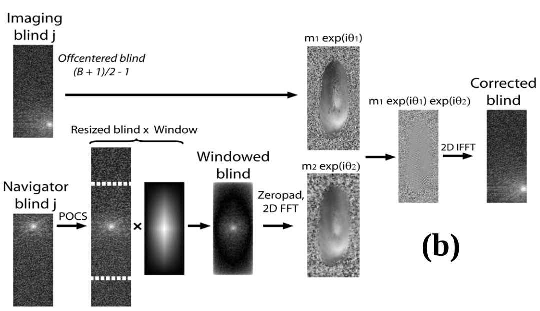

Figure 2: (a) Summary of the reconstruction steps applied to the partial Fourier RS-EPI *b* = 0 and diffusion-weighted data. A fully-sampled central blind provides a central segment for FOV/2-ghost correction and GRAPPA calibration. Individual interleaves of each blind are now complex-averaged to form a single blind. A 2D FFT is applied to each blind, and gridding (9) of the partial Fourier data is performed to combine all blinds in *k*-space. POCS reconstruction is performed for each coil to fill in the remaining extent of *k*-space. After an inverse FFT, the final image is produced by combining images from all coils via performing the sum of squares. (b) Triangular phase correction process applied to each partial Fourier diffusion-weighted blind in RS-EPI.

Materials & Methods: The RS-EPI spin echo-based (twice-refocused) diffusion pulse sequence timing diagram is shown in Fig. 1. For each TR, an imaging echo (or 'blind') and its accompanying navigator echo are acquired. Each navigator echo is used only to sample the central blind of *k*-space. The imaging echo fills *k*-space with separate (adjacent or overlapping) blinds until the target resolution is reached. Depending upon the number of blinds chosen, *B*; the blind width, *W*; and the target resolution *N* (in the readout-direction) – the amount the blinds may overlap, *dW*, is described by the *overlapping factor*, *OF*. In the case of parallel imaging, only the central blind is acquired, using a GRAPPA-acceleration factor of *R* = NEX. This blind can be used for referenceless Nyquist ghost parameter estimation (2) and GRAPPA (3-4) calibration, values which are applied to all other (*b* = 0 and DW blinds). A summary of the steps used to reconstruct the partial Fourier GRAPPA-accelerated RS-EPI data is shown in Fig. 2a. For the navigator (phase) correction, each navigator is windowed in *k*-space by a triangular function used for PROPELLER DWI (5,6) prior to Fourier transformation (FFT). This removes all low-frequency spatially varying phase in image space for each blind (6). There are three apparent differences between the phase correction of PROPELLER and that of RS-EPI (see Fig. 2b). Firstly, RS-EPI is not self-navigated, therefore the phase of a blind is removed from the phase of the accompanying windowed navigator (rather than from the phase of a windowed version of the blind itself). Secondly, to preserve the distance of the blind relative to the *k*-space center for off-centered blinds, they cannot be individually reconstructed with partial Fourier reconstruction (this step is instead performed after gridding). Rather, the navigator undergoes partial Fourier (POCS) reconstruction (7,8), and the high-spatial frequency blind edges are discarded, to a size equivalent to that of the imaging blind. This provides a phase map that can be used for correction. Thirdly, because the navigator phase is inverted due to the 180º pulse, the phase correction step is a multiplication rather than a division. All scans were performed on a 3T whole-body GE EXCITE system (Milwaukee, WI, USA; G = 40 mT/m, SLR = 150 mT/m/s) using an eight-channel head coil. Datasets were acquired on a healthy volunteer. To provide a dataset with which to test various overlapping factors, GRAPPA-accelerated RS-EPI images were acquired with and without peripheral cardiac gating at in-plane target resolutions of 288 x 288 using *B* = 33 blinds of width 64 (*OF* = 86%). The acquisitions consisted of one *b* = 0 s/mm^2 and one *b* = 1000 s/mm^2 applied in the S/I direction. Three repetitions of the non-gated experiment were made. Other imaging parameters were as follows: *R* (=NEX) = 3; TE = minimum (68 ms); number of overscans (N_O) = 18; TR = 3 RR intervals (gated), TR = 3 s (non-gated acquisitions); and *FOV* = 24 cm. All RS-EPI datasets were reconstructed with the use of the navigator correction outlined in Fig. 2b. For both acquisitions, the 33 acquired blinds were reconstructed with varying *OF*s.

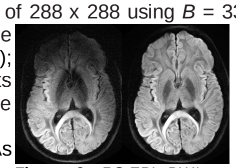

Figure 3: RS-EPI DWI non-gated datasets (*b*=1000 s/mm^2, S/I direction) acquired with *N* = 288, *R* =*NEX*=3, N_O = 18, *W*=64, *OF*=36%, FOV = 24 cm, slthck = 5 mm, TR = 3s and a scan time = 2:10 min (incl. *b*=0). (left) without, and (right) with phase correction.

Results: Fig. 3 shows non-gated DW-RS-EPI datasets (*B* = 33*, OF* = 86%) reconstructed without and with navigator correction. As shown, navigator correction corrects for the majority of phase shifts/ghosting artifacts that occur between blinds, resulting in considerably improved SNR. Fig. 4 shows navigator-corrected gated and non-gated datasets reconstructed with various blind overlapping factors. As shown, ignoring the loss of SNR with decreasing overlapping factor, even adjacent (*OF* = 0 %) blinds are robust to artifacts due to physiological motion.

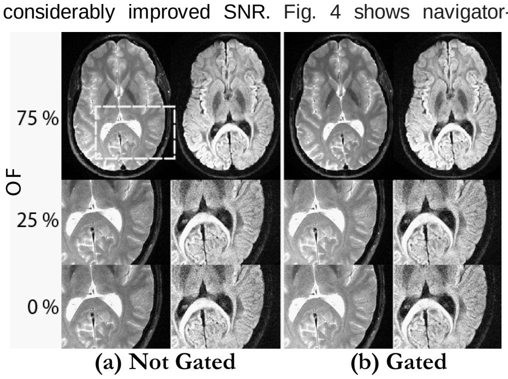

Figure 4: RS-EPI diffusion-weighted navigator-corrected datasets (*b* = 1000 s/mm^2, S/I direction) acquired (a) with and (b) without gating at a target resolution of 288 x 288. The datasets are reconstructed with different overlapping factors as shown.

Discussion: In this abstract, the navigator-corrected non-gated DW-RS-EPI acquisitions rendered images with comparable quality compared with gated acquisitions. However, in the case of severe brain motion, this may not rule out the possibility of complete signal dropout of the central blind. A practical way to reduce this risk would be to increase the number of overscans and acquire one-two extra center blinds. Ignoring these signal voids, there seems to be considerable flexibility in the choice of overlapping factor. This work shows that RS-EPI acquisitions can be used without cardiac gating and with adjacent blinds. However, if *k*-space shifts due to involuntary patient motion are of concern then it may be sensible to use *OF* > 0%. Scan time permitting, a higher overlapping factor can also be selected if a higher SNR is desired. It is shown here that patient handling can be simplified with the use of non-gated acquisitions, enabling the acquisition of high resolution DW images with minimal distortion in a clinically relevant scan time. The criteria for minimally overlapping blinds (reduced scan time) may make this sampling strategy a useful alternative to other methods used for navigated DW imaging.

References: 1) Porter ISMRM 2004;442. 2) Nordell ISMRM 2007:1833. 3) Griswold MRM 2002;47:1202-1210. 4) Qu JMR 2005;174(1):60-67. 5) Pipe MRM 1999;42(5):963-969. 6) Pipe MRM 2002;47(1):42-52. 7) Haacke JMR 1991;92:126-145. 8) Liang Rev MRM 1992;4:67-185. 9) Jackson IEEE TMI 1991;10:473-478. **Acknowledgements:** This work was supported in part by the NIH (2R01EB002711, 1R21EB006860), the Center of Advanced MR Technology at Stanford (P41RR09784), Lucas Foundation, Oak Foundation, and the Swedish Research Council (K2007-53P-20322-01-4).